

## **On the weldability and corrosion resistance of alloy UNS N08827 – a further improvement of alloy UNS N08825**

Julia Botinha  
VDM Metals International GmbH  
Kleffstraße 23  
Altena, 58762  
Germany

Martin Wolf  
VDM Metals International GmbH  
Kleffstraße 23  
Altena, 58762  
Germany

Helena Alves  
VDM Metals International GmbH  
Kleffstraße 23  
Altena, 58762  
Germany

### **ABSTRACT**

As described in recently published papers, the nickel-based alloy UNS<sup>(1)</sup> N08827, commercially known as alloy 825 CTP, has been developed to fill in the existing gap between alloys UNS N08825 and UNS N06625. It is an austenitic nickel based alloy composed mostly by nickel, iron and chromium with additions of molybdenum and copper. In comparison to UNS N08825, UNS N08827 has doubled molybdenum content, which grants to this alloy a higher localized corrosion resistance, as well as no titanium additions, which significantly improves the weldability. In comparison to UNS N06625, UNS N08827 has a lower nickel content, which assures commercial advantage.

In this paper, we present the most recent corrosion test results of UNS N08827 as a base material, as well as of welded coupons. The mechanical and corrosion properties of welded parts are compared with the same properties of the base material. Corrosion test results according to ASTM<sup>(2)</sup> G48 Methods C and D and ASTM G28 Practice A are provided. The experiments conclude that UNS N08827 has improved corrosion resistance in comparison to UNS N08825 and that welded products do have comparable corrosion properties as the base material.

**Key words:** UNS N08827, UNS N08825, Alloy 825, localized corrosion, intergranular corrosion, weldability

---

<sup>(1)</sup> Unifying Numbering System

<sup>(2)</sup> American Society for Testing and Materials, West Conshohocken, Pennsylvania, USA

© 2023 Association for Materials Protection and Performance (AMPP). All rights reserved. No part of this publication may be reproduced, stored in a retrieval system, or transmitted, in any form or by any means (electronic, mechanical, photocopying, recording, or otherwise) without the prior written permission of AMPP.

Positions and opinions advanced in this work are those of the author(s) and not necessarily those of AMPP. Responsibility for the content of the work lies solely with the author(s).

## INTRODUCTION

Recently, the nickel-based alloy UNS N08827, commercially known as VDM ® Alloy 825 CTP<sup>(3)</sup>, has been presented to the oil and gas industry as an alloy that has been developed to fill in the existing gap between both UNS N08825 and UNS N06625 in terms of localized corrosion resistance.<sup>1,2,3</sup> It is a solid-solution nickel alloy with chemical composition similar to UNS N08825, except for its doubled molybdenum content and the no addition of titanium.

The molybdenum content of 4.5 to 6.5 % grants to UNS N08827 a higher localized corrosion resistance in comparison to UNS N08825 (2.5 to 3.5 %), mainly in chloride-containing environments. This feature is well known and can be verified by the Pitting Resistance Equivalent Number (PREN), which is given by equation 1, where molybdenum has a factor of 3.3, meaning its importance to the alloy protection against localized corrosion.

$$PREN = 1 \times \%Cr + 3.3 \times (\%Mo + 0.5 \times \%W) + 16 \times \%N \quad (\text{Eq. 1})$$

UNS N08825 has been developed in the 50's,<sup>4</sup> when the available manufacturing routes did not allow for carbon contents as low as they are possible nowadays. Elements like titanium and niobium have been usually added to solid solution alloys to stabilize the carbon and prevent precipitation of chromium carbides in the grain boundaries. Chromium carbides sequester the chromium available in the matrix and lead to chromium depletion in the region close to its precipitation location, the grain boundaries, where the alloy may be more prone to corrosion attack. A minimum limit of 0.6 wt-% titanium is defined in the composition requirements of UNS N08825.<sup>5</sup>

In counterpart, the presence of titanium can result in some challenges in terms of weldability. As well as titanium has affinity with the carbon as described before, it also has a very high affinity with the nitrogen, forming titanium nitrides. Despite the limited information available in the literature regarding the effects of titanium on the weldability of nickel alloys, some authors have reported some of its effects. A high titanium enrichment along cracks and interdendritic regions has been observed by Shankar et al.<sup>6</sup> They report that titanium tends to segregate in grain boundaries, leading to the formation of a higher density of detrimental secondary phases in this region, what can later contribute to the formation and propagation of cracks. Another effect of titanium cited in the literature is related to its effect to the solidification intervals. Lippold mentions that the partitioning of titanium to boundary areas significantly drops the solidification temperature at these sites, increasing the solidification intervals, what might lead to hot cracking occurrence.<sup>7</sup> During arc welding, titanium may also form stable oxides due to its unpredictable oxidation behavior, leading to a possible depletion of interstitial titanium, thus reducing its stabilization effect.

In a recent publication, solidification intervals of UNS N08825, N08827 and N06625 have been calculated for different cooling rates using the thermodynamic calculation software JMatPro<sup>(4)</sup>, where the solidification intervals of UNS N08827 are between the both of N08825 and N06625.<sup>3</sup>

## EXPERIMENTAL PROCEDURE

### Autogenous Plasma Arc Joint Welds

For the assessment of the joint weldability, plasma arc weldings (PAW) were carried out using 5 mm plates of UNS N08827 with ground surface finishing. Argon with a degree of purity higher than

---

<sup>(3)</sup> Trade name.

<sup>(4)</sup> Trade name. Java-based Materials Properties.

99.996 % was chosen as backing gas. The PAW was used as an autogenous process, which means that no filler material was added. The used welding parameters are given on Table 1.

The welded joints were metallographically examined using optical techniques and corrosion tested according to ASTM G48 Methods C and D in the as-welded condition, as well as after a simulated post weld heat treatment at 625 °C for 8 hours followed by water-cooling.

**Table 1**  
**Autonomous plasma arc welding parameters**

Arc current	220 A
Arc Voltage	19.5 V
Travel speed of the torch	30 cm/min (11.8-in/min)
Plasma gas flow rate	1 L/min
Shielding gas flow rate	20 L/min
Working distance	5 mm (0.2-in.)

### **Welded tubes**

Welded tubes of 10 mm diameter and 1.2 mm wall thickness were produced by a partner using an autogenous plasma welding process. Figure 1 shows a picture of one sample of the produced tube. The welded tube was tested for its critical pitting temperature (CPT) according to ASTM G48 Method C.<sup>8</sup> The chosen start temperature was 30 °C, since this is the temperature at which UNS N08825 shows pitting corrosion. Due to limitation of material availability, the test was successfully performed using the same tube sample, containing the weld seam, and the temperature was increased for each test step by 5 °C.

A crevice testing according to the same norm, Method D, was not possible due to geometrical limitations.



**Figure 1: Autogenous plasma welded tube made of UNS N08827 plate**

### **Welding with filler metal addition – characterization of welded material**

A welding joint was created using several subsequent welding passes in order to produce a weld seam large enough to accommodate several testing coupons (all-weld-metal samples). The welding passes were carried out according to the sketch shown on Figure 2. The applied welding process was manual GTAW using TIG rods with a diameter of 2.40 mm (0.095-in). The applied welding parameters were 12 to 14 Volts, 160 Amps and a welding speed of 14 – 16 cm/min (5.5 - 6.3 in/min.). The shielding gas was Ar with a purity of 99.996%.

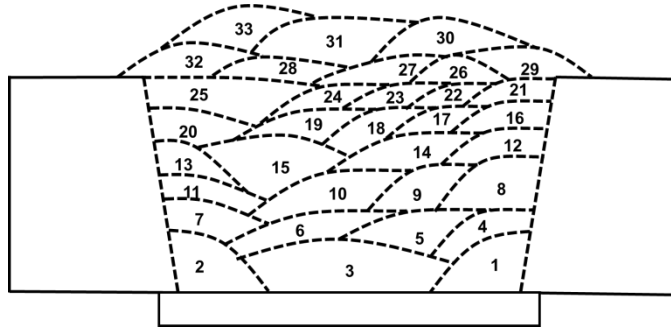


**Figure 2: Sketch of welding passes to create weld material for further testing**

After the weld was finished, samples have been taken from weld seam only to have the filler material analyzed for its chemical composition, mechanical and corrosion properties.

The chemical composition was analyzed through optical emission spectroscopy (PA II SPETROLAB<sup>(5)</sup> Ni 2016) with the sample preparation according to DIN EN ISO 14284:2003<sup>9</sup>. Tensile tests at room temperature were carried out according to DIN EN ISO 6892-1<sup>10</sup> with tensile samples taken longitudinally to the weld seam. Charpy impact tests were carried out according to DIN EN ISO 148-1<sup>11</sup> and DIN EN ISO 9016<sup>12</sup> at room temperature and at -196 °C. The corrosion properties were investigated through ASTM G48 Method C, to define the critical pitting temperature of the weld metal, and ASTM G28 Practice A, to investigate the intergranular corrosion behavior of the weld metal.

#### Modified Varestraint-Transvarestraint (MVT) Tests

For comparing the filler metal UNS N08827 to its predecessor UNS N08825 (FM 65) concerning hot cracking susceptibility during welding, the externally loaded Modified Varestraint Transvarestraint (MVT) hot cracking test was applied according to ISO/TR 17641-3:2005<sup>13</sup>. Due to the MVT test procedure, the all-weld-metal samples were autonomously re-welded using GTAW with an energy input per unit length of 7.5 kJ/cm and with bending strains of 1 %, 2 % and 4 %. After the test, the samples were analyzed in a stereo microscope and potential hot cracks were differentiated between solidification cracks, liquation cracks and ductility dip cracks. All three kinds of hot cracks were counted and the solidification as well as the liquation cracks were measured to their lengths.

The results were then plotted in a total-crack-length versus strain diagram, where the materials are grouped into sectors that define their hot cracking tendency as “vulnerable to cracking”, “with increasing tendency to cracking” and “hot crack safe”.

The MVT tests were performed at the BAM<sup>(6)</sup>.

For investigating the overlay weld capabilities of the filler metal UNS N08827, a mock-up component test was performed. For this reason a seamless carbon steel tube (EN 10204 P355J2H) with a diameter of 254 mm (10 in) and wall thickness 25.0 mm (0.98 in) was spirally weld cladded using the GTAW cold wire process. The applied welding parameters are listed in Table 2.

#### Mock-Up Test

The overlay welding onto the carbon steel tube was performed at a tube length of ca. 350 mm (13.8 in.) with one layer, at a tube length of ca. 200 mm (7.8 in.) with two layers and at a tube length of 50 mm

<sup>(5)</sup> Trade name

<sup>(6)</sup> Bundesanstalt für Materialforschung und –prüfung (BAM), Unter den Eichen 87 12205 Berlin, Germany.

© 2023 Association for Materials Protection and Performance (AMPP). All rights reserved. No part of this publication may be reproduced, stored in a retrieval system, or transmitted, in any form or by any means (electronic, mechanical, photocopying, recording, or otherwise) without the prior written permission of AMPP.

Positions and opinions advanced in this work are those of the author(s) and not necessarily those of AMPP. Responsibility for the content of the work lies solely with the author(s).

(2.0 in) with multiple layers resulting in a total weld metal height of 43 mm (1.7 in). Afterwards the tube was cut into pieces and metallographic as well as hardness specimens were dissected.

**Table 2**  
**GTAW parameters for overlay welding**

Arc current	220 A
Arc Voltage	13.6 V
Travel speed of the torch	80 cm / min (31.5 in/min)
Wire feeding speed	5.10 m/min. (200.8 in/min)
Shielding gas	Ar (99.996)
Shielding + trailing gas flow rate	20 L/min
Weld position	flat

## RESULTS

### Autogenous Plasma Arc Joint Welds

Figure 3 shows an optical metallography of the weld joint carried out transversal to the weld seam. Additional views were made in detail on the weld seam, heat affected zone and base material close to the weld. No nitrides, oxides, pores or cracks could be identified. Few to no precipitation in the grain boundaries and inside the grains could be identified.

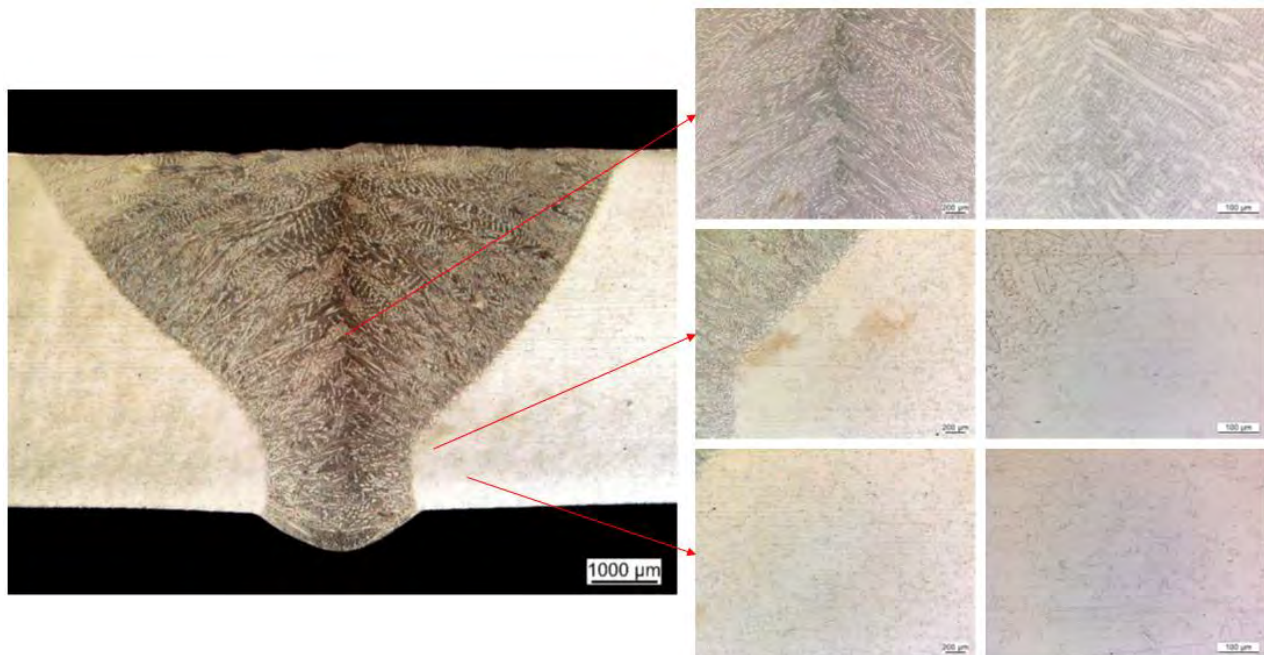


**Figure 3: Transversal metallography view of weld seam with detailed regions**

In Table 3 the CPT and CCT of the welded joint in the as-welded condition and after simulated post weld heat treatment (SPWHT) are shown.

**Table 3**  
**Critical pitting temperature and pitting crevice temperature of autogenous PAW plates according to ASTM G48 C and D in the as-welded condition and after SPWHT**

Test Method	Condition	CPT (°C)	CCT (°C)
ASTM G48 C	As-welded	50	-
ASTM G48 C	Welded+SPWHT	50	-
ASTM G48 D	As-welded	-	35
ASTM G48 D	Welded+SPWHT	-	30

### Welded Tubes

The results of the ASTM G48 C test carried out in the sample of welded tube are shown on Table 4. The CTP determined for the welded tube sample of alloy 825 CTP is 55 °C and it is defined as being the minimum temperature to produce pitting attack on the surface of the specimen.

Although the pitting corrosion has mostly initiated in the weld seam, as shown by Figure 4, the temperature at which it starts being observed is similar to the ones observed for the base material and therefore we can conclude that there is no detrimental effect of the welding process in the pitting corrosion resistance of UNS N08827.

**Table 4**  
**Results of ASTM G 48 C test to define the critical pitting temperature of welded-tube made of UNS N08827**

Test temperature °C	Test duration hours	Weight difference grams	Mass loss rate mm/a	Pit
30	24	0.00	0.0	No
35	24	0.00	0.0	No
40	24	0.00	0.0	No
45	24	0.00	0.0	No
50	24	0.00	0.0	No
55	24	0.59	15.6	Yes



**Figure 4: Sample of welded tube tested according to ASTM G48 Method C at 55 °C, after pitting corrosion took place in the surface of the sample**

### Welding with filler metal addition – characterization of welded material

The cross section of weld seam as well as micrographs showing the seam and heat affected zone in detail are shown in Figure 5. Even after several welding passes, no nitrides, oxides, pores or cracks

could be identified in the weld seam and few to no precipitation in the heat-affected zone could be identified.

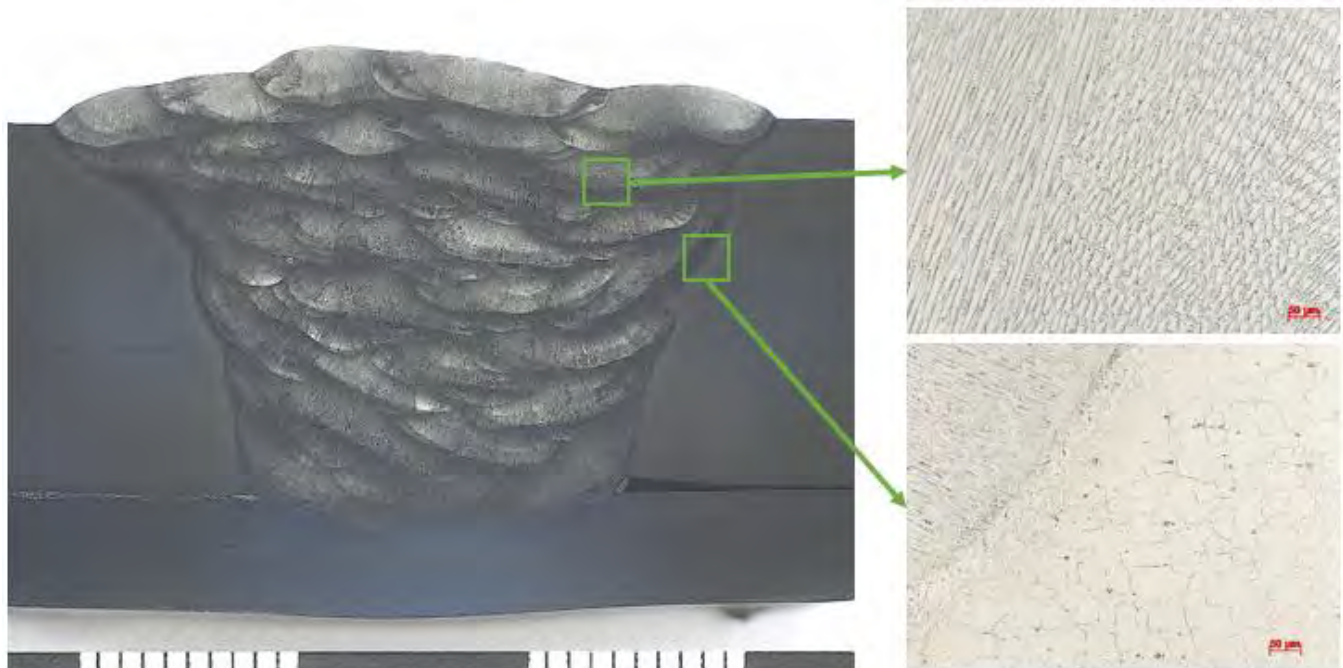


**Figure 5: Cross section showing the structure of weld seam after several welding passes and micrographs showing the weld seam and heat affected zone**

The chemical analysis of the weld metal 825 CTP can be found on Table 5 together with the chemical requirements of UNS N08827 and the chemical composition of the filler metal used for this trial. The chemical composition of the material does not change significantly after welding, presenting only a slight carbon uptake, although it remains on a very low level. Since the samples for chemical analysis were taken from some distance to the edge of the welding seam, it is not expected that the base metal has an influence on its chemical composition.

**Table 5  
Chemical composition of UNS N08827, filler metal 825 CTP and its weld metal**

		C	Si	Mn	S	Al	Ti	Cu	Cr	Mo	B	Fe	Co
UNS N08827	Min	-	0.2	0.5	-	0.06	-	1.6	21.0	4.5	0.002	Bal.	-
	max	0.015	0.5	0.9	0.005	0.25	0.1	2.3	23.0	6.5	0.004		0.5
Filler metal		0.002	0.26	0.69	0.002	0.11	0.06	2.02	22.39	5.76	0.002	29.0	0.18
Weld metal		0.004	0.24	0.68	0.003	0.10	0.07	1.97	22.40	5.86	0.003	29.0	0.14

The tensile and impact properties of the weld metal are shown on Table 6. The minimum requirements for the base material are also given in this table as a reference, as well as properties of a reference heat of base material of UNS N08827. The weld metal of UNS N08827 has tensile and toughness properties in accordance to the base metal requirements.

The corrosion results of tests carried out on weld metal are shown on Table 7. The CPT is 50 °C and is comparable to the CPT of the base metal available in the literature.<sup>3</sup> The intergranular corrosion rates are very low and comparable with common values that are seen for UNS N08825.

**Table 6**  
**Tensile and Charpy impact toughness of weld metal**

Sample	Temp.	Rp0.2	Rp1.0	TS	Elongation	RoA	Ay (J)		
	(°C)	(MPa)	(MPa)	(MPa)	(%)	(%)	1	2	3
Minimum UNS N08827	RT	241	-	586	30	-	-	-	-
Base material	RT	320	-	667	50	80	-	-	-
Base material	-196	-	-	-	-	-	277	278	237
T1	RT	439	468	624	35.0	65	-	-	-
T2	RT	441	472	624	35.5	71	-	-	-
C1	RT	-	-	-	-	-	250	235	281
C2	-196	-	-	-	-	-	201	214	220

**Table 7**  
**Corrosion results of weld metal**

Corrosion test	Sample Nr.	Test period (h)	CPT (°C)	Corrosion rate (g/m <sup>2</sup> h)	Corrosion rate (mm/a)
ASTM G48 C	1	72h per cycle	50	-	-
	2	72h per cycle	50	-	-
ASTM G28 A	1	120	-	0.1643	0.176
	2	120	-	0.1723	0.184

### Modified Varestraint-Transvarestraint (MVT) Tests

Samples of both welded metal UNS N08825 (FM 825) and N08827 (FM 825 CTP) were investigated through MVT tests to assess their susceptibility to hot cracking. After welding, the total crack length of each sample was calculated and plotted on the diagram shown on Figure 6.

The results show that, as expected by the calculated solidification intervals, FM 825 CTP presents much less cracks after welding in comparison to FM 825. As it can be seen, the diagram of Figure 6 can be divided in 3 sectors, each indicating a different behavior to hot cracking while/after welding: 1) hot crack safe, 2) with increasing tendency to hot cracking and 3) vulnerable to cracking.

FM 825 CTP finds itself in the sector 1, which indicates that the filler metal is hot crack safe, while FM 825 finds itself right over the line that divides both sectors 2 and 3, indicating that this filler metal has an increased tendency to hot cracking or might be vulnerable to cracking.

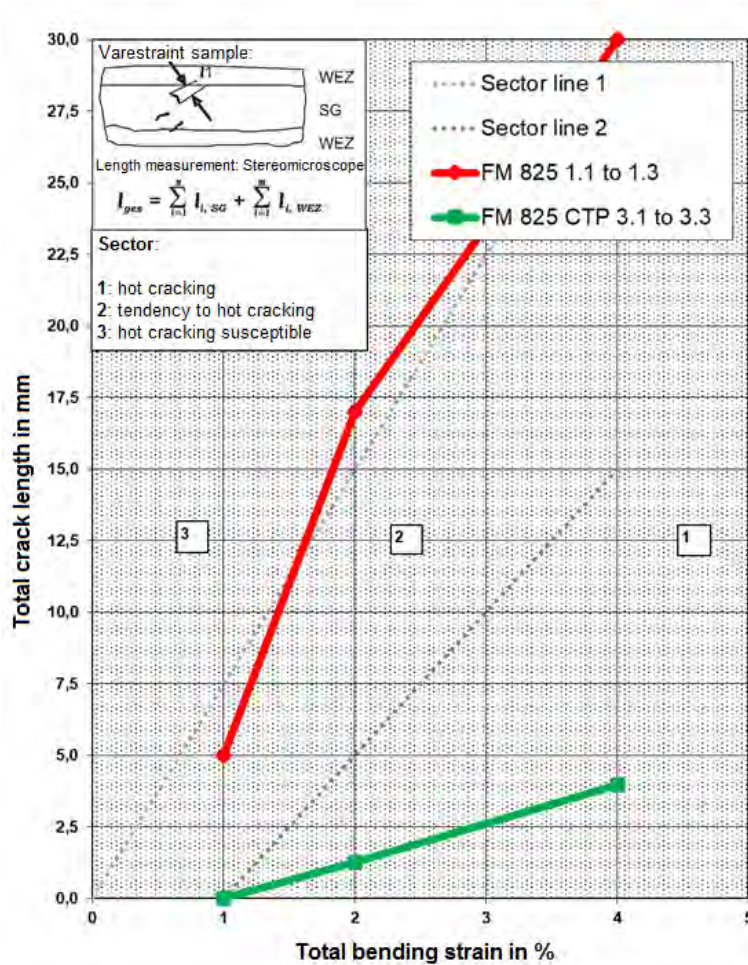
### Mock-Up Test

Figure 7 shows the mock-up overlay weldment during the dye penetration testing according to DIN EN ISO 3452. The dye penetration test indicated no cracks or other notable flaws like pores or lack of fusion (LoF).

The clad tube was then cut to size for carrying out metallographical investigations and hardness measurements. Figure 8 shows the metallographic samples and the metallographic results according to DIN EN ISO 17639<sup>14</sup>. The metallographic results show that no significant flaws like macro or micro



cracking could be found in the cross section validating the negative finding of the previously done dye penetration testing.



**Figure 6: Influence of the bending strain in the total crack length of the weld metal samples of FM 825 CTP and FM 825. Sector 1 means hot crack safe, sector 2 means with increasing tendency to cracking and sector 3 means vulnerable to cracking**



**Figure 7: Mock-up overlay welding of a tube**

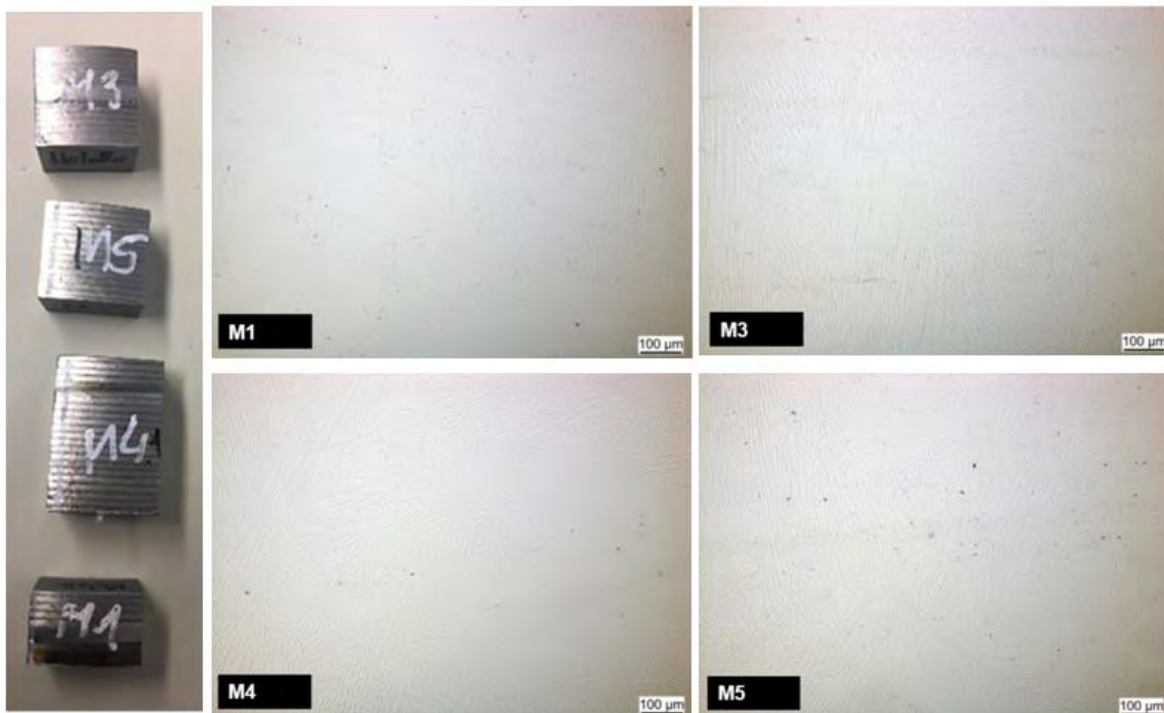
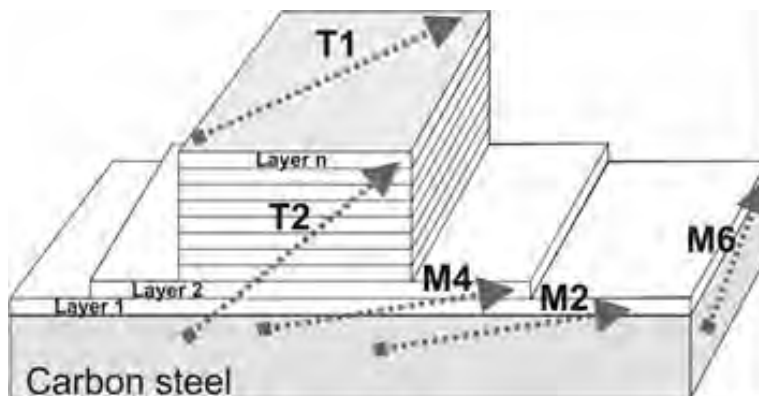


**Figure 8: Preparation of the metallographic samples and results (unetched condition)**

Vickers hardness traces were measured according to DIN EN ISO 9015<sup>15</sup> on the basis of ISO 15614-7<sup>16</sup>. The values are given in the table of Figure 9. The values show that the hardness of the weld metal N08827 (nearly undiluted T1) is in the range of 229 to 252 HV10. According to the literature, cladded UNS N06625 presents hardness of about 300 to 400 Vickers.<sup>17</sup> In comparison to UNS N06625, the hardness of N08827 is significantly less thus facilitating the machining of cladded surfaces with N08827.



HV 10 Measurement / according to ISO 15614-7																
Specimen	Value 1	Value 2	Value 3	Value 4	Value 5	Value 6	Value 7	Value 8	Value 9	Value 10	Value 11	Value 12	Value 13	Value 14	Value 15	Value 16
T1	233	245	252	235	237	245	235	235	234	229	238					
T2	184	192	228	220	243	236	243	223	229	223	235	223	227	225		
M2	166	173	173	174	178	184	185	200	257	334	196	170				
M4	177	180	182	186	188	190	193	199	215	278	292	270	199	199	188	187
M6	193	199	206	205	208	206	233	288	284	295	300	211	193	185		
	FM 825 CTP - Weld metal					HAZ Carbon steel			Carbon steel BM							

**Figure 9: Determination of the hardness from carbon steel to the UNS N08827 and of the weld metal N08827 only**

## CONCLUSIONS

The results of the welding program carried out using UNS N08827 base material and filler metal show that the chemical composition of UNS N08827 allows its welding without the development of hot cracking and/or the precipitation of detrimental phases to the weld joint.

The mechanical as well as the corrosion properties of weld metal, as well as of autogenous welded samples, are similar to the properties of the base material, showing that this alloy does not lose any corrosion or mechanical resistance after being welded.

## ACKNOWLEDGEMENTS

The authors would like to specially thank Sebastian Maus and Roland Wachtmann for carrying out the corrosion tests at the laboratories of VDM Metals.

## REFERENCES

1. J. Klöwer, J. Rosenberg. "The corrosion behavior of an advanced version of alloy UNS N08825". Houston, TX : NACE Corrosion Conference 2017, 2017. C2017-9334.
2. J. Botinha, G. Genchev, J. Krämer, C. Bosch, H. Alves. "Effect of Sensitization on the Corrosion Resistance of an Advanced Version of Alloy UNS N08825". Houston, TX : NACE Corrosion 2019, 2019. C2019-12729.
3. J. Botinha, M. Wolf, B. Gehrman, H. Alves. "Alloy UNS N08827: a New and Advanced Version of Alloy UNS N08825 with Better Corrosion and Hot Cracking Resistance". Houston, TX : NACE Corrosion 2021, 2021. C2021-16398.
4. S. Thompson, J. McIntyre. Special Metals Corporation: Innovator of the future celebrates 100 years of excellence. Stainless Steel World. May 2006.
5. International, ASTM. ASTM B424-19 Standard Specification for Nickel-Iron-Chromium-Copper Alloys Plate, Sheet and Strip. 2019.
6. V. Shankar, T.P.S. Gill, A.L.E. Terrance, S.L.Mannan and S. Sundaresan. Relation between Microstructure, Composition, and Hot Cracking in Ti-Stabilized Austenitic Stainless Steel Weldments. s.l. : Metallurgical and Materials Transactions A, Volume 31 A, p. 3109-3122, 2000.
7. J. C. Lippold, An Investigation of Weld Cracking in Alloy 800. s.l. : Welding research supplement, p. 91-103. Bd. March 1984.
8. ASTM G48 - 11 Standard Test Methods for Pitting and Crevice Corrosion Resistance of Stainless Steels and Related Alloys by Use of Ferric Chloride Solution. ASTM International. West Conshohocken, PA 19428-2959 United States : s.n., 2015.
9. DIN EN ISO 14284:2003 "Steel and iron - Sampling and preparation of samples for the determination of chemical composition".
10. DIN EN ISO 6892-1:2020-06 "Metallic materials - Tensile testing - Part 1: Method of test at room temperature" (ISO 6892-1:2019).
11. DIN EN ISO 148-1:2017-05 "Metallic materials - Charpy pendulum impact test - Part 1: Test method" (ISO 148-1:2016).
12. DIN EN ISO 9016:2013-02 "Destructive tests on welds in metallic materials - Impact tests - Test specimen location, notch orientation and examination" (ISO 9016:2012).
13. ISO/TR 17641-3:2004 "Destructive tests on welds in metallic materials - Hot cracking tests for weldments - Arc Welding Processes - Part 3: Externally loaded test". 2005.

14. DIN EN ISO 17639:2022 "Destructive tests on welds in metallic materials - Macroscopic and microscopic examination of welds" (ISO 17639:2022); German version EN ISO 17639:2022.
15. DIN EN ISO 9015 "Destructive tests on welds in metallic materials - Hardness testing - Part 1: Hardness test on arc welded joints" (ISO 9015-1:2001); German version EN ISO 9015-1:2011.
16. ISO 15614-7 "Specification and qualification of welding procedures for metallic materials - Welding procedure test - Part 7: Overlay welding" (ISO 15614-7:2016); German version EN ISO 15614-7:2016.
17. T. Dai, R.A. Wheeling, K. Hartmann-Vaeth and J.C. Lippold. "Precipitation behavior and hardness response of Alloy 625 weld overlay under different aging conditions. International Institute of Welding, 2019.
18. DIN EN ISO 9016:2013-02 "Destructive tests on welds in metallic materials - Impact tests - Test specimen location, notch orientation and examination" (ISO 9016:2012).